

## Supplementary materials for "Geologic versus geodetic deformation adjacent to the San Andreas fault, central California"

by S. Titus et al., revised for Geological Society of America Bulletin, February, 2010.

### Summary

This supplementary document provides additional information about all of the GPS station velocities used in this study. Our description of the station velocities is sub-divided into sites located in undeforming areas of the Sierra Nevada-Great Valley block (SNGV), sites located on the Pacific plate, and sites located within deforming areas adjacent to the San Andreas fault.

### GPS data processing

All station velocities used in this study were determined from GIPSY-OASIS II analysis at the University of Wisconsin-Madison of the original GPS code-phase data. Daily station positions through May 10 of 2009 were determined using release 4.02 of GIPSY and satellite products from the Jet Propulsion Laboratory. The latter consist of the standard non-fiducial (*e.g.* \*\_nf.eci, \*\_nf.tdpc, etc...) files produced by JPL between the 1990s and mid-2009. The satellite products do not include the newer generation orbits from JPL that have been generated since early 2009 and which are meant for use with release 5.0 of GIPSY.

Best-fitting slopes, intercepts, and antenna offsets were estimated from inversions of the coordinate time series for all sites, with additional corrections (described below) at some sites to reduce the influence of coseismic and postseismic motion from the 2003 San Simeon and 2004 Parkfield earthquakes on their velocity estimates.

All of the GPS station locations are specified in ITRF2005 (Altamimi et al. 2007). Following Argus (2007), we adopt the Earth's center-of-mass as the appropriate origin for geodetically described plate motions. Argus (2007) estimates that Earth's center-of-mass moves relative to the ITRF2005 geocenter at respective rates of  $0.3 \text{ mm yr}^{-1}$ ,  $0.0 \text{ mm yr}^{-1}$ , and  $1.2 \text{ mm yr}^{-1}$  in the X, Y, and Z directions. Opposite-sense corrections are therefore made to all of the GPS station velocities to offset the motion of ITRF2005 relative to the Earth's center-of-mass.

### Sierra Nevada-Great Valley block motion

Figure 1 shows the locations of the 32 GPS stations we used to estimate the angular velocity of the Sierra Nevada-Great Valley (SNGV) block relative to ITRF2005. We identified 32 continuous stations from nominally stable areas of the SNGV block (shown by the red arrows in Fig. 1) and inverted their velocities (given in Table 1) to estimate the angular velocity for the SNGV block relative to ITRF2005. The best-fitting angular velocity ( $8.0^\circ\text{S}$ ,  $111.9^\circ\text{W}$ ,  $0.289^\circ \text{ Myr}^{-1}$ ) fits the 32 station velocities well (Figure 1), with reduced chi-square of 1.3 and weighted mean residual motions of  $0.64 \text{ mm yr}^{-1}$  and  $0.68 \text{ mm yr}^{-1}$  in the north and east velocity components, respectively. The misfits to the station velocities are only slightly larger (by 10%) than the estimated velocity uncertainties.

### Pacific plate motion

We estimate the angular velocity of the Pacific plate relative to ITRF2005 from the velocities of 27 stations (Figure 2 and Table 2). Absent any compelling evidence for deformation within the Pacific plate, we used as many station velocities as possible, including three sites from the eastern Pacific basin (GUAX, CLAR, and SOCC), and stations in the southern, western, and central Pa-

cific. Twenty-five of the 27 stations are continuous (Table 2). Data from campaign sites CLAR and SOCC in the eastern Pacific (Marquez-Azua et al. 2004) span 3.1 years and 7.3 years, respectively.

The best-fitting Pacific plate angular velocity ( $63.5^{\circ}\text{S}$ ,  $110.7^{\circ}\text{E}$ ,  $0.676^{\circ}\text{ Myr}^{-1}$ ) fits the 27 station velocities well, with weighted mean residual motions of  $0.71\text{ mm yr}^{-1}$  and  $0.94\text{ mm yr}^{-1}$  in the north and east components, respectively. These compare well with previously reported misfits for Pacific plate station velocities (Beavan et al. 2002; Plattner et al. 2007). Reduced chi-square for the 27 Pacific plate station velocities is 2.0, indicating that the velocity misfits exceed their uncertainties by 40% on average. Although the higher than expected misfits could be evidence for internal deformation of the Pacific plate, the WRMS values for the Pacific plate station velocities are only modestly higher than for other plates with abundant GPS station velocities. We thus suspect that the station velocity uncertainties are modestly under-estimated.

The wide geographic area spanned by the 27 station velocities imposes strong constraints on the angular velocity, as has been the case for previous studies. For example, our best-fitting pole ( $63.5^{\circ}\text{S}$ ,  $110.7^{\circ}\text{E}$ ) lies within 0.5 angular degrees of poles estimated by Beavan et al. (2002) and Plattner et al. (2007) even though all three Pacific plate angular velocity estimates are referenced to different versions of the international terrestrial reference frame. The preferred Pacific plate angular velocities for the three studies predict Pacific plate motion that differs by only fractions of a  $\text{mm yr}^{-1}$  within the study area in central California, too small to affect any of the results or conclusions reached herein.

### **Deforming areas adjacent to the San Andreas fault**

Table 3 gives the motions of the 150 stations from the study area in central California and Figure 3 shows their residual velocities in reference frames fixed to the Pacific plate and SNGV block. Below, we use the time series of two continuous stations from the study area to illustrate the effects of the  $M_w=6.6$  December 22, 2003 San Simeon and  $M_w=6.2$  September 28, 2004 Parkfield earthquakes on deformation in the study area and to illustrate our procedures for reducing the effect of these two earthquakes on our estimates of the interseismic station velocities.

### **GPS station velocities: Central California**

Station QCYN, which is located 25 km southwest of the creeping segment of the San Andreas fault and 50 km or farther from the epicenters of both the San Simeon and Parkfield earthquakes, moved southward by 11 mm and westward by 3 mm during the 2003 San Simeon earthquake (Fig. 4), consistent with the coseismic elastic deformation associated with this earthquake (Rolandone et al. 2006). During the months following the earthquake, QCYN moved an additional 2-3 mm to the south (Figs. 4 and 5), but appears to have resumed its steady interseismic motion by the middle of 2004. During the 2004 Parkfield earthquake, the coseismic motion at QCYN was only 3 millimeters to the north and west, near the lower detection limit for this station.

An inversion of the daily station positions at QCYN to estimate the slopes and intercepts that best describe the north and east components of the station motion before the San Simeon earthquake and after mid-2004 gives best slopes of  $4.9\text{ mm yr}^{-1}$  to the south and  $1.7\text{ mm yr}^{-1}$  to the east after removing Pacific plate motion (Fig. 5). In contrast, an inversion of the daily positions from January 1, 2007 to mid-2009, several years after both earthquakes occurred, gives best slopes of  $5.3\text{ mm yr}^{-1}$  to the south and  $1.3\text{ mm yr}^{-1}$  to the east after removing Pacific plate motion (Fig. 6). The difference in the station velocities for these two time intervals is only  $0.6\text{ mm yr}^{-1}$ , smaller than their  $\pm 1.2\text{ mm yr}^{-1}$  combined  $1-\sigma$  uncertainty. Any change in the velocity at QCYN due to postseismic effects of the San Simeon and Parkfield earthquakes is thus too small to detect.

Station PKDB is located southwest of the San Andreas fault and 20 km from the epicenter of the 2004 Parkfield earthquake. The station exhibits significantly larger coseismic and postseismic responses to the San Simeon and Parkfield earthquakes than does station QCYN (Figure 7). A visual examination of the station time series indicates that the 2004 Parkfield earthquake triggered a protracted postseismic response that affected the station motion for years after the earthquake, possibly to the present (Figure 8). Our inversion to estimate the best long-term rate at this site therefore excludes all station positions from Dec. 22, 2003 to the start of 2007, by which time most of the postseismic motion from the 2004 Parkfield earthquake appears to have occurred. The remaining station positions, extending from 1996 to mid-2009 are best fit by rates of  $6.6 \text{ mm yr}^{-1}$  to the south and  $6.9 \text{ mm yr}^{-1}$  to the east after removing Pacific plate motion (Figure 8).

Given our concern that slow postseismic motion continued to affect the motion at station PKDB after early 2007 (Figure 9), we inverted the station positions for the period from early 2007 to mid-2009 to estimate the station velocity. The best-fitting station velocity is  $2.1 \text{ mm yr}^{-1}$  faster than, but parallel to, the longer-term average rate described above. The speed-up in station motion is consistent with the large amount of afterslip observed after the 2004 Parkfield earthquake (Johanson et al. 2006) and strongly suggests that afterslip continued to affect the secular, interseismic velocity field near Parkfield after 2007.

We also analyzed the position time series (not shown) for station CRBT, which is located midway between the San Simeon and Parkfield earthquakes at respective distances of 33 km and 35 km from their epicenters. Encouragingly, the long-term rate we determine from a joint inversion of the station positions for the periods mid-2001 to Dec. 22, 2003 and Jan. 1, 2007 to mid-2009 differs by only  $0.6 \text{ mm yr}^{-1}$  from the rate we determined for the period Jan. 1, 2007 to mid-2009. The small difference once again suggests that any bias in our estimate of the long-term station rate due to postseismic motions associated with either of these earthquakes is small.

A rigorous treatment of the postseismic effects of the San Simeon and 2004 Parkfield earthquakes at all stations in central California is beyond the scope of this work. As is described below, we estimated and applied corrections for the coseismic and postseismic effects of these two earthquakes at all the continuous and campaign sites in our study area. Our analysis of the motion at station PKDB suggests that biases in the velocities of stations within 20 km of one or both of those rupture zones could be as large as several  $\text{mm yr}^{-1}$  despite our attempt to estimate and correct for the postseismic effects of the earthquakes. Caution is thus warranted in interpreting the motions of stations near the Parkfield rupture zone and possibly the San Simeon rupture zone in the context of long-term deformation. In contrast, our analyses of the motions at stations QCYN and CRBT, which are located 30 km or farther from the epicenters of the San Simeon and 2004 Parkfield earthquakes, reveal no measurable, protracted postseismic effect from either earthquake. Our estimates of the interseismic motions of most stations located 30 km or farther from the two rupture zones are thus likely to be accurate to within  $1 \text{ mm yr}^{-1}$ , absent other significant sources of error in their velocity estimates.

### **Continuous station velocity estimates**

We determined long-term interseismic velocities of continuous GPS stations in central California from inversions of their daily station positions, including estimates of the magnitude of any antenna offsets. Data from the time of the San Simeon earthquake (Dec. 22, 2003) until no sooner than mid-2004 and no later than Dec. 31, 2006 were excluded from the inversion to minimize the coseismic and postseismic effects of the San Simeon and Parkfield earthquakes.

### **Campaign stations:**

At each of our campaign sites, we applied corrections to the station position time series using elastic displacements calculated from the best-fitting distributions of coseismic fault-slip and postseismic fault-afterslip for the San Simeon earthquake (Rolandone et al. 2006) and Parkfield earthquake (Johanson et al. 2006). The corrections, shown in Figure 10, range in magnitude from 65 millimeters for stations close to the earthquake rupture zones to only 1-2 millimeters at more distant sites and depend strongly on the location of each station relative to the two earthquake rupture zones.

We assessed the possible effect of these corrections on our campaign site velocity estimates by comparing offsets that we estimated from the time series of five continuous GPS stations in the study area that were operating during both earthquakes (CRBT, GR8V, MEE1, MEE2, and QCYN) to the elastic corrections predicted for the San Simeon and Parkfield earthquakes (Fig. 10). The modeled corrections typically agree with the observed offsets to within 3 millimeters. Given that most of the campaign site observations span time periods of four years or longer (Table 3), the misfits of 3 mm or smaller imply that biases in our estimates of the interseismic site velocities are likely to be  $1 \text{ mm yr}^{-1}$  or less, too small to affect any of our major conclusions. The good agreement between the interseismic velocities we estimate for the campaign sites and those estimated for nearby continuous sites further suggests that both sets of velocities approximate the long-term interseismic deformation in this region.

### **References**

Altamimi, Z., Collilieux, X., Legrand, J., Garayt, B., and Boucher, C., 2007, ITRF2005: A new release of the International Terrestrial Reference Frame based on time series of station positions and Earth Orientation parameters *Journal of Geophysical Research*, v. 112, no. B09401, doi:10.1029/2007JB004949.

Argus, D. F., 2007, Defining the translational velocity of the reference frame of Earth, *Geophysical Journal International* v. 169, p. 830–838, doi: 10.1111/j.1365-246X.2007.03344.x.

Beavan, J., Tregoning, P., Bevis, M., Kato, T., and Meertens, C., 2002, Motion and rigidity of the Pacific plate and implications for plate boundary deformation, *Journal of Geophysical Research* v. 107 (B10), doi:10.1029/2001JB000282.

Johanson, I. A., Fielding, E. J., Rolandone, F., and Burgmann, R., 2006, Coseismic and postseismic slip of the 2004 Parkfield earthquake from space-geodetic data, *Bulletin of the Seismological Society of America*, v. 96, S269–S282, doi:10.1785/0120050818.

Marquez-Azua, B., Cabral-Cano, E., Correa-Mora, F., and DeMets, C., 2004, A model for Mexican neotectonics based on nationwide GPS measurements, 1993-2001, *Geofisica Internacional*, v. 43, p. 319–330.

Plattner, C., Malservisi, R., Dixon, T. H., LaFemina, P., Sella, G., Fletcher, J., and Vidal-Suarez, F., 2007, New constraints on relative motion between the Pacific plate and Baja California microplate (Mexico) from GPS measurements, *Geophysical Journal International*, v. 170, p. 1373-1380, doi:10.1111/j.1365-246X.2007.03494.x.

Rolandone, F., Dreger, D., Murray, M., and Burgmann, R., 2006, Coseismic slip distribution of the 2003  $M_w$  6.6 San Simeon earthquake, California, determined from GPS measurements and seismic waveform data, *Geophysical Research Letters*, v. 33, L16315, doi: 10.1029/2006GL027079.



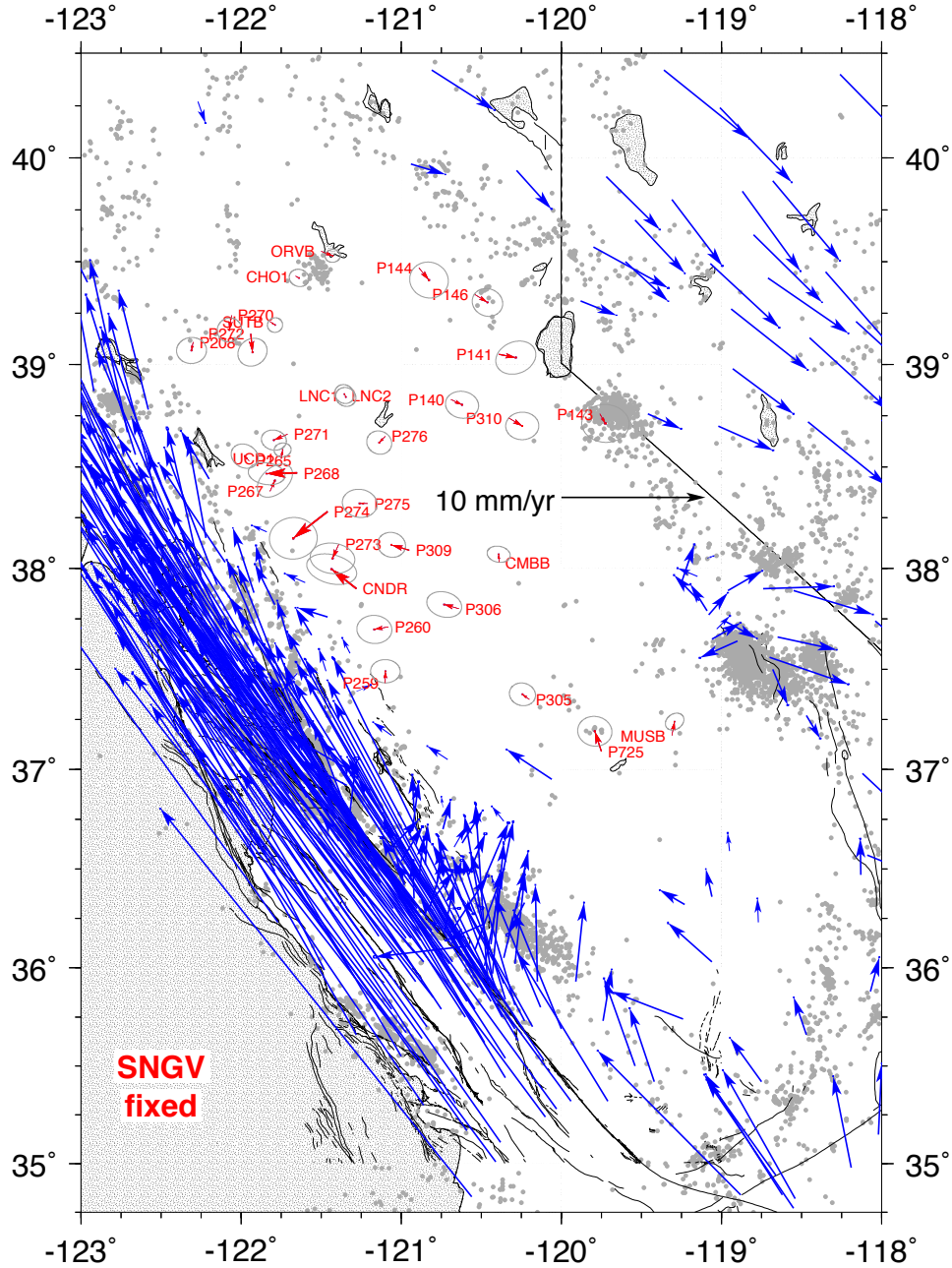


Figure 1: Residual velocities for stations on the Sierra Nevada-Great Valley (SNGV) block (red) and other stations (blue) within the map area after subtracting the velocity predicted by the best-fitting SNGV-ITRF2005 angular velocity given in the text. Uncertainty ellipses are 2-D, 1- $\sigma$ . Each residual site velocity is determined by subtracting the motion predicted at the site by the angular velocity that best describes the motion of the SNGV block relative to ITRF2005 from the site motion measured relative to ITRF2005. All station velocities are corrected for the motion of the geocenter, as described above. Station velocities are given in Table 1.

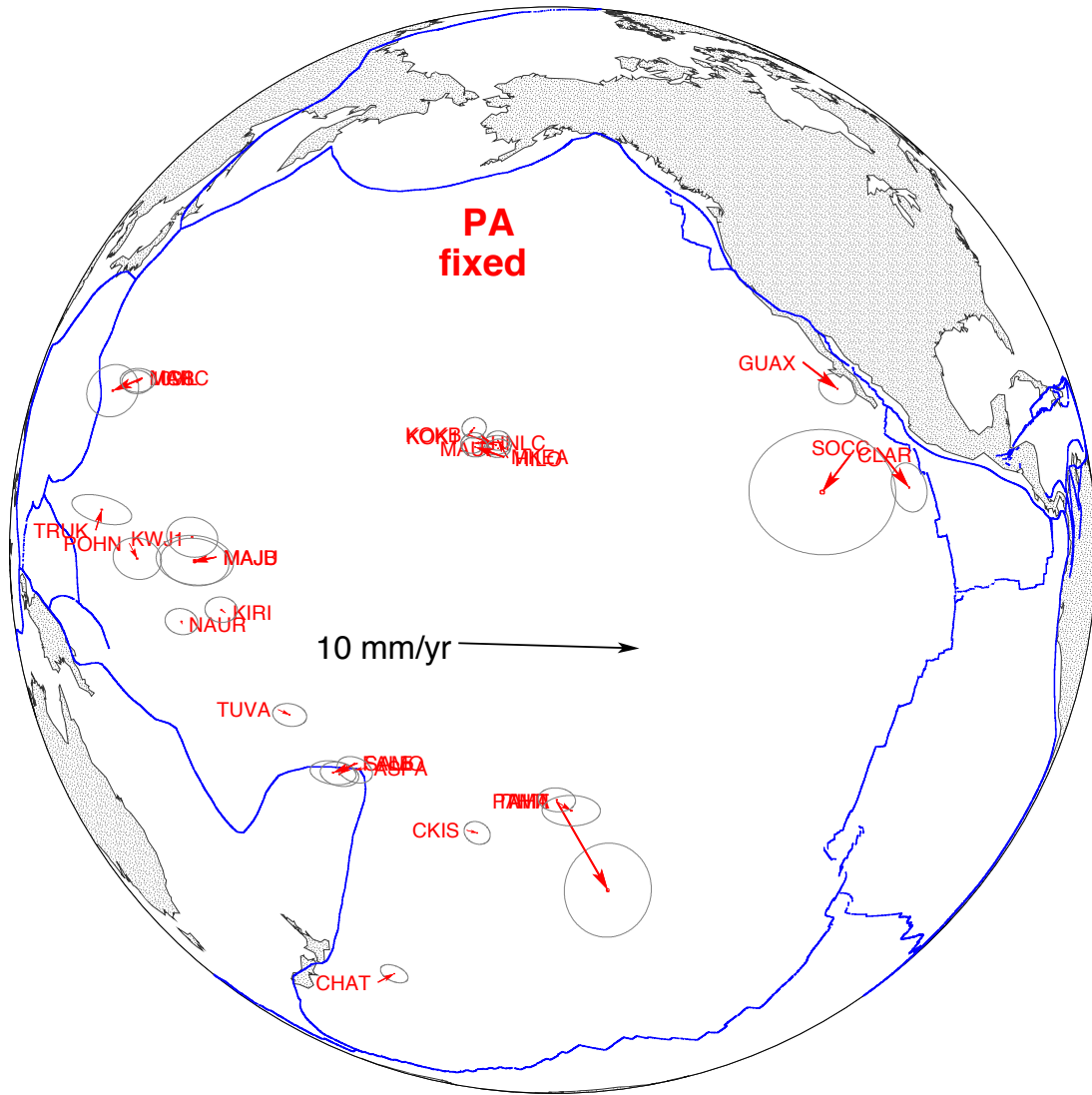


Figure 2: Residual velocities for 27 Pacific plate stations with their 2-D, 1- $\sigma$  uncertainty ellipses. Each residual site velocity is determined by subtracting the linear velocity predicted at the site by the angular velocity that best describes the motion of the Pacific plate relative to ITRF2005 from the site velocity relative to ITRF2005. All station velocities are corrected for the motion of the geocenter, as described in the text. Station velocities are given in Table 2.

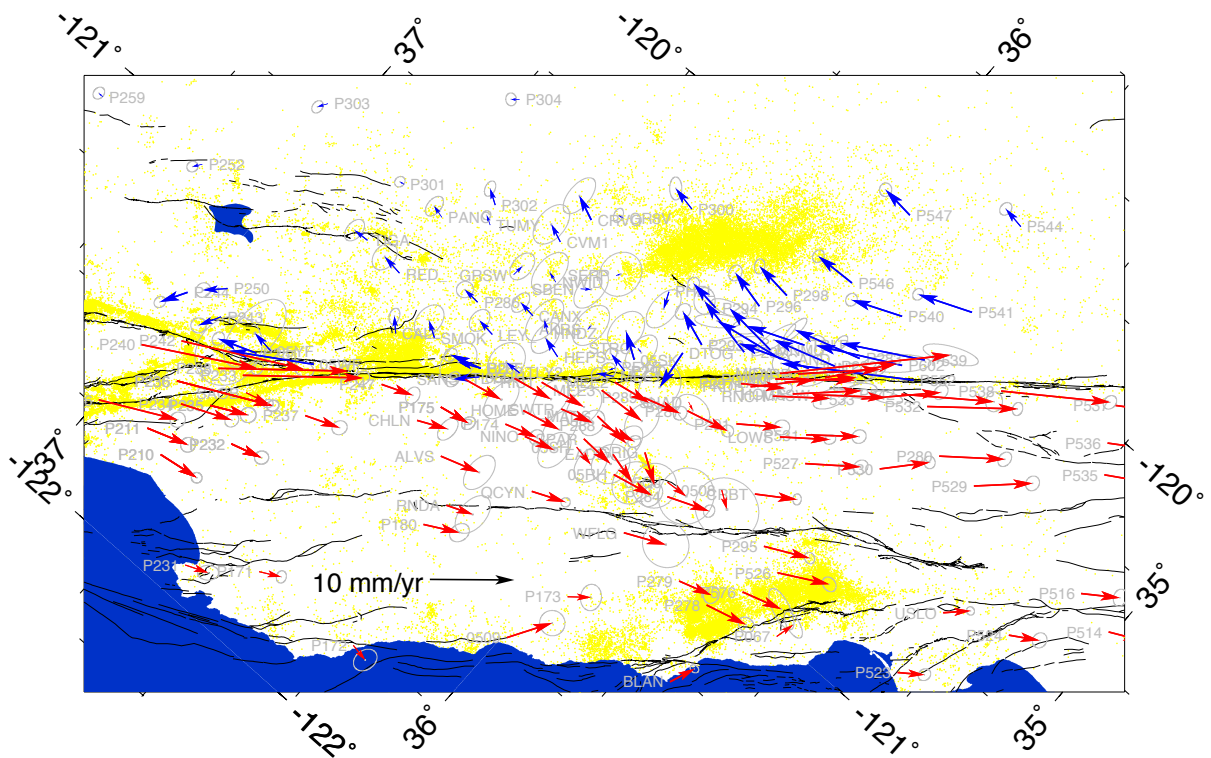


Figure 3: Residual velocities of stations in central California relative to the SNGV block (blue) and Pacific plate (red). Uncertainty ellipses are 2-D, 1- $\sigma$ . The azimuth of the projection equator is N41°W. Residual motions show the measured station motion relative to ITRF2005 reduced by the motion that is predicted by the angular velocity that best describes the motion of the SNGV block relative to ITRF2005. All station velocities are corrected for motion of the ITRF2005 origin relative to Earth’s center-of-mass, as described in the text. Earthquakes with magnitude above 1.0 are shown by yellow symbols and are for the period 1972 to 2009. The station velocities relative to ITRF2005 are given in Table 3.



QCYN reduced site motion ( 36.161N 238.863E)

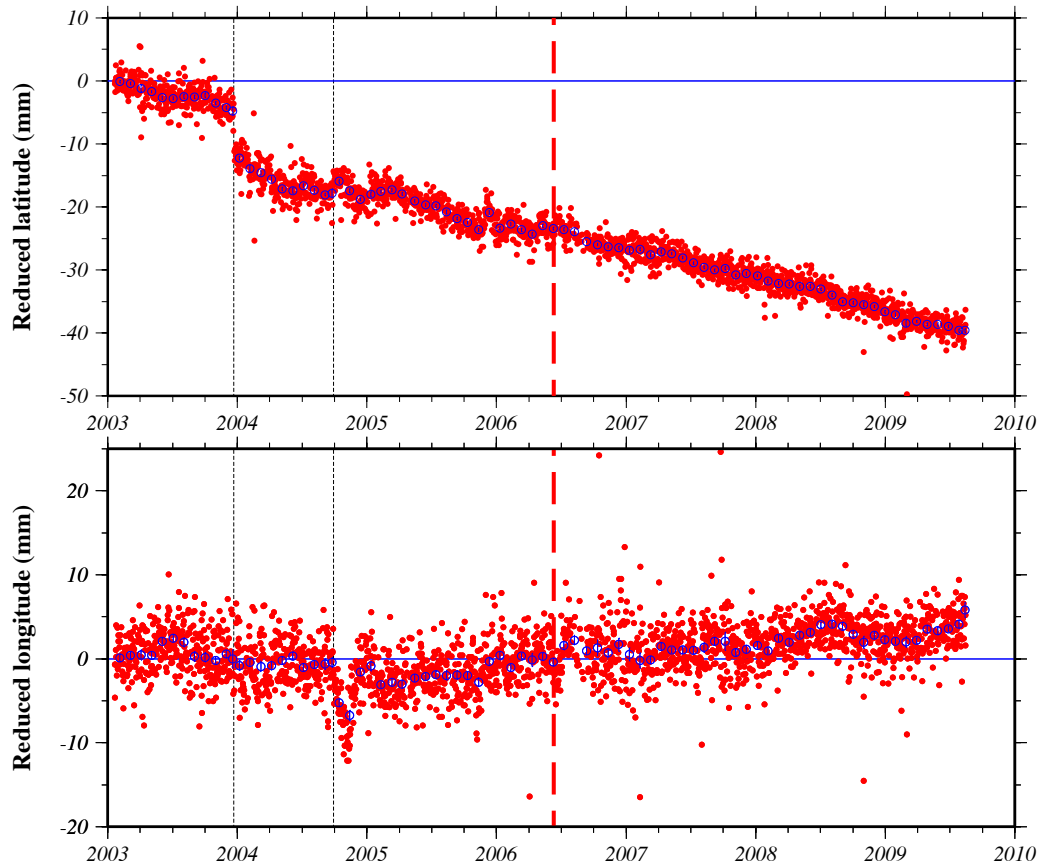


Figure 4: Uncorrected north and east movements of station QCYN adjacent to the central creeping segment of the San Andreas fault in millimeters from 2003 to mid-2009 after removal of Pacific plate motion. Red and blue circles show daily and weekly station position estimates, respectively. No other corrections to the coordinate time series have been made. Dotted vertical lines indicate the times of the Dec. 22, 2003 San Simeon and Sept. 28, 2004 Parkfield earthquakes. Bold red line indicates the time that the GPS monument was moved by several tens of meters to a new monument.

QCYN reduced site motion ( 36.161N 238.863E)

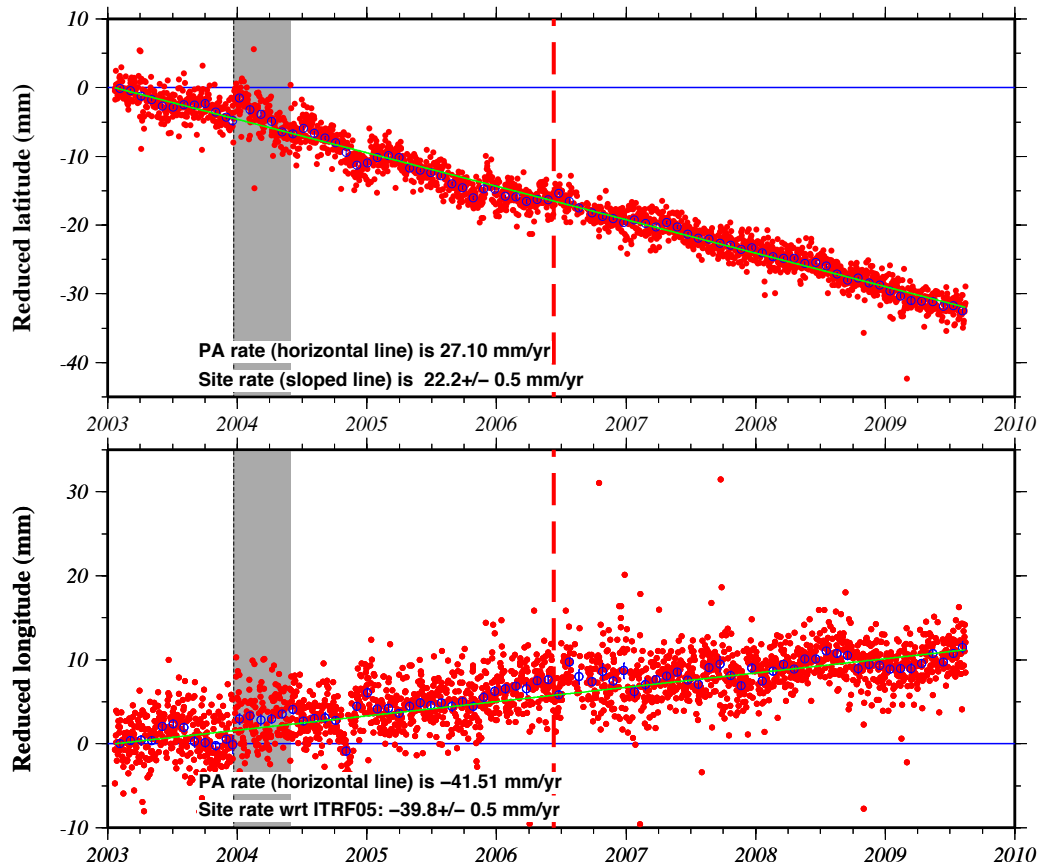


Figure 5: Linear regression of daily north and east components positions for station QCYN to find best-fitting slope, intercept, and offsets for the 2003 San Simeon and 2004 Parkfield earthquakes. Pacific plate motion is removed from the station coordinates. Shaded region indicates station positions that are excluded from the determination of the best-fitting slope and intercept. Red and blue circles show daily and weekly station position estimates, respectively. Dotted vertical lines indicate the times of the Dec. 22, 2003 San Simeon and Sept. 28, 2004 Parkfield earthquakes.

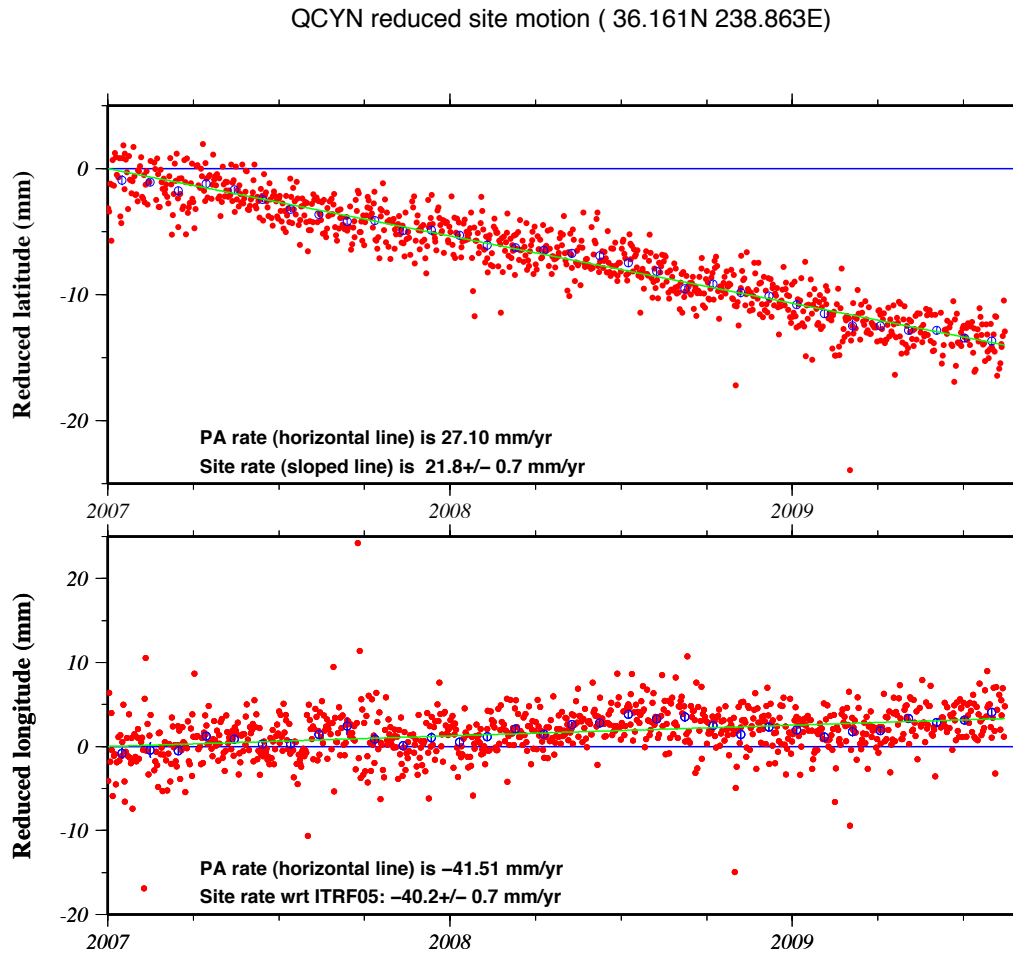


Figure 6: Linear regression of daily north and east components positions for the period Jan. 1, 2007 to mid-2009 for station QCYN to find best-fitting slope and intercept. Pacific plate motion is removed from the station coordinates. Red and blue circles show daily and weekly station position estimates, respectively.

PKDB reduced site motion ( 35.945N 239.458E)

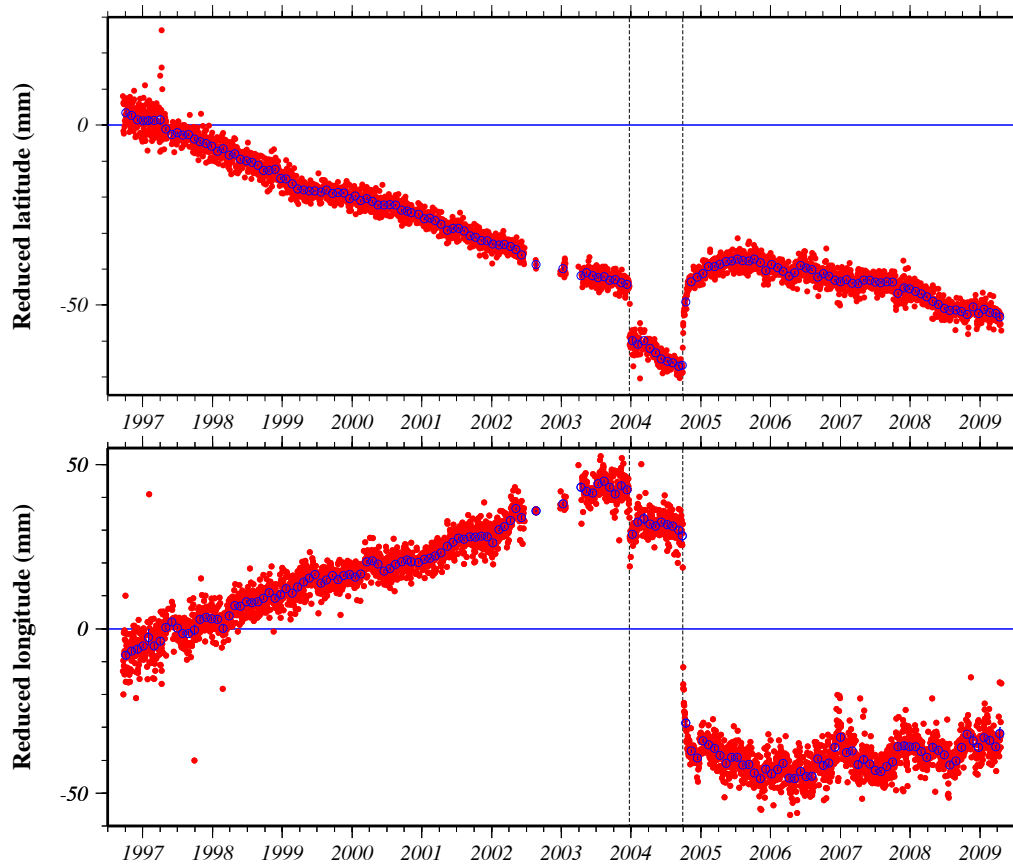


Figure 7: Uncorrected north and east movements of station PKDB adjacent to the Parkfield segment of the San Andreas fault in millimeters from 1996 to mid-2009 after removal of Pacific plate motion. Dotted vertical lines indicate the times of the Dec. 22, 2003 San Simeon and Sept. 28, 2004 Parkfield earthquakes. Red and blue circles show daily and weekly station position estimates, respectively.

PKDB reduced site motion ( 35.945N 239.458E)

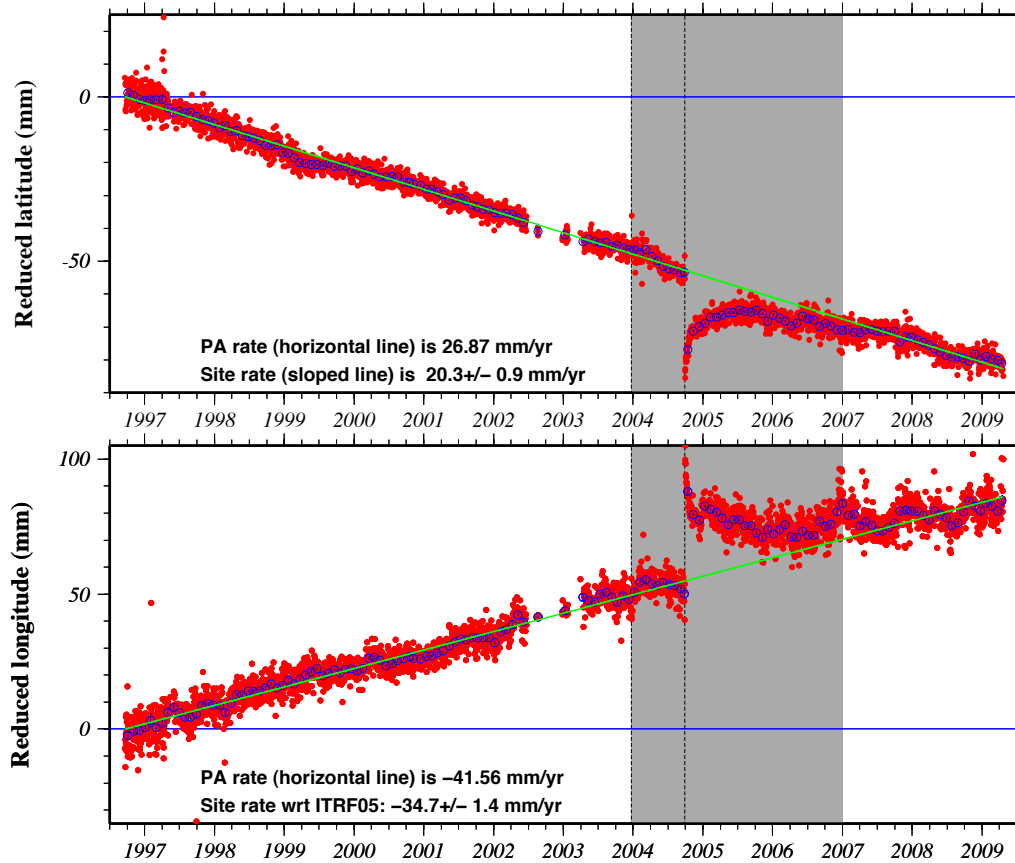


Figure 8: Linear regression of daily north and east components positions for station PKDB adjacent to the Parkfield segment to find best-fitting slope, intercept, and offsets for the 2003 San Simeon and 2004 Parkfield earthquakes. Pacific plate motion is removed from the station coordinates. Shaded region indicates station positions that are excluded from the determination of the best-fitting slope and intercept. Red and blue circles show daily and weekly station position estimates, respectively. Dotted vertical lines indicate the times of the Dec. 22, 2003 San Simeon and Sept. 28, 2004 Parkfield earthquakes.

PKDB reduced site motion ( 35.945N 239.458E)

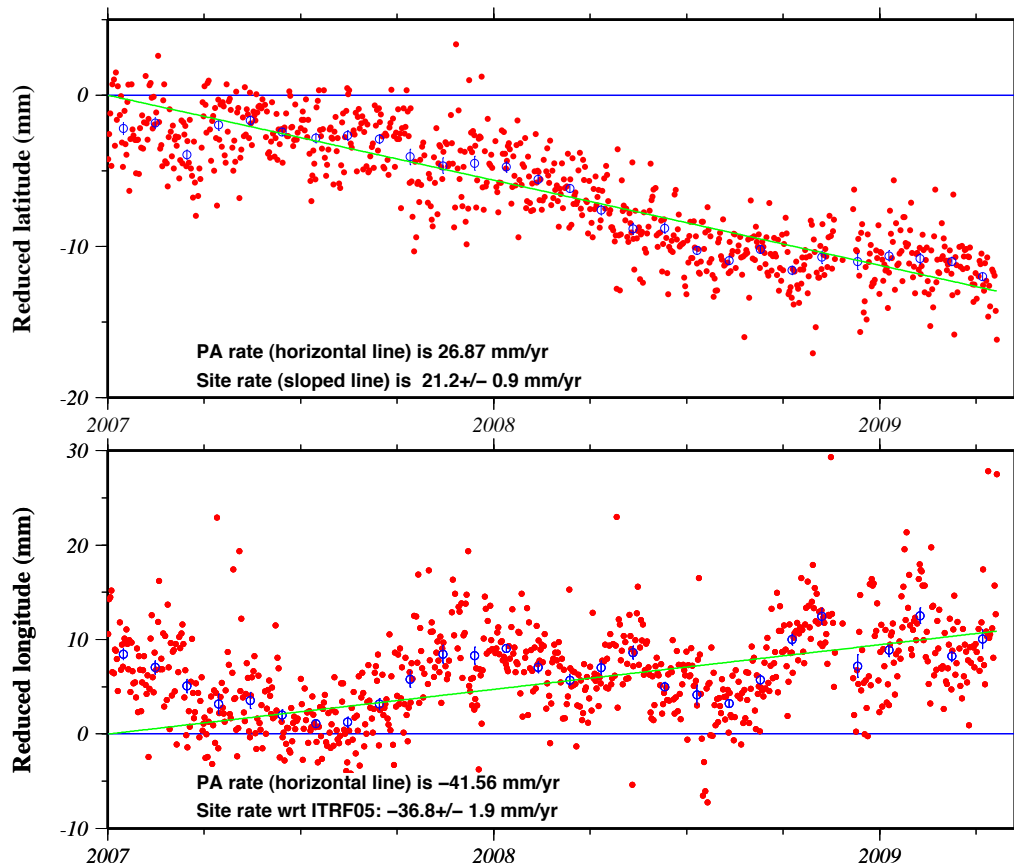


Figure 9: Linear regression of daily north and east components positions for the period Jan. 1, 2007 to mid-2009 for station PKDB near Parkfield to find best-fitting slope and intercept. Pacific plate motion is removed from the station coordinates. Red and blue circles show daily and weekly station position estimates, respectively.

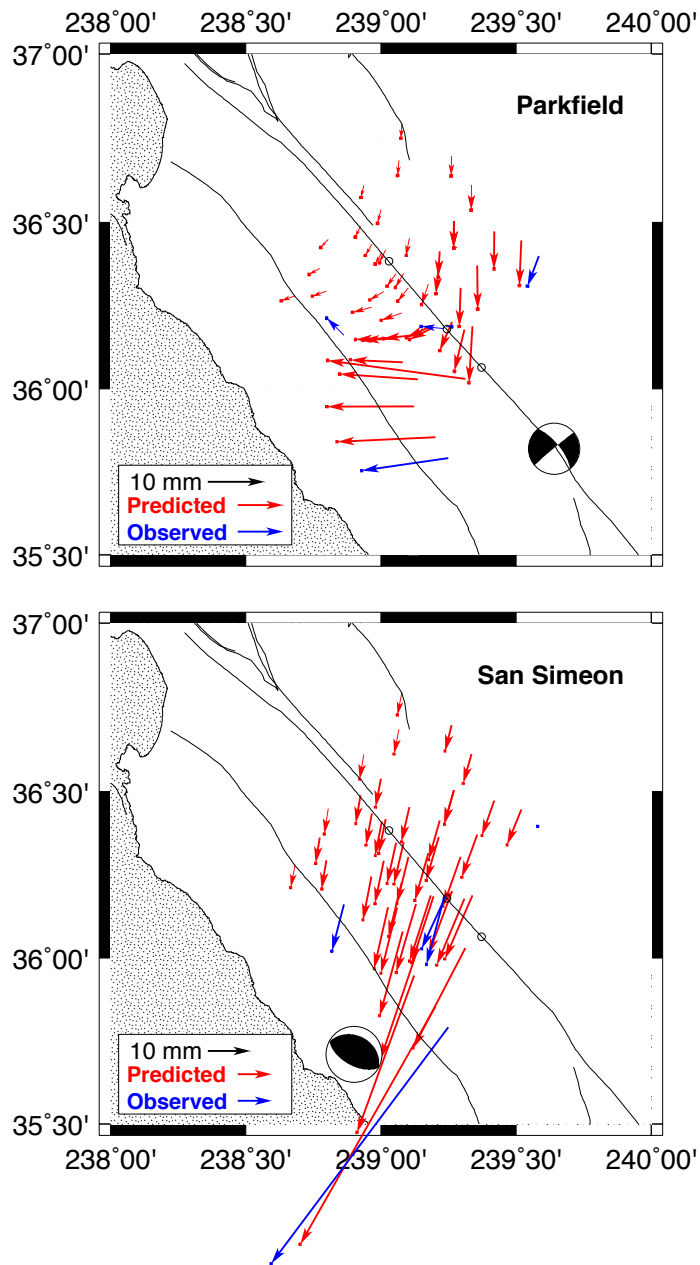


Figure 10: *Upper* - Combined coseismic and postseismic displacement for the 2004 Parkfield earthquake predicted by the best-fitting elastic half-space model of Johanson et al. (2006) (red) and coseismic displacements (blue) measured at continuous stations along the central creeping segment of the San Andreas fault. Displacements are predicted at the locations of all the campaign stations included in the study area. *Lower* - Combined coseismic and postseismic displacement for the 2003 San Simeon earthquake predicted by the best-fitting elastic half-space model of Rolandone et al. (2006) (red) and coseismic displacements (blue) measured at the same four continuous stations.

Table 1: GPS station information: Sierra Nevada-Great Valley block

Site code	Lat. °N	Long. °W	$V_e$ mm yr <sup>-1</sup>	$V_n$ mm yr <sup>-1</sup>	Corr. coeff.	Station days	Time yrs	First obs.
CHO1	39.433	121.665	-22.7±0.5	-4.5±0.4	-0.11	2704	8.5	1999.54
CMBB	38.034	120.386	-22.5±0.6	-3.1±0.4	-0.18	4697	15.4	1993.94
CNDR	37.896	121.278	-24.1±1.2	-2.8±0.7	-0.28	1494	6.9	1999.29
LNC1	38.847	121.350	-22.7±0.5	-4.3±0.4	-0.09	1853	5.7	2003.63
LNC2	38.847	121.351	-22.8±0.5	-4.1±0.4	-0.11	363	5.7	2003.63
MUSB	37.170	119.309	-22.0±0.4	-2.1±0.4	0.14	3514	11.5	1997.85
ORVB	39.555	121.500	-22.2±0.3	-4.6±0.3	0.04	4067	12.5	1996.89
SUTB	39.206	121.821	-22.5±0.4	-4.7±0.3	-0.00	3670	12.1	1997.24
UCD1	38.536	121.751	-22.5±0.4	-3.8±0.3	0.06	3229	13.0	1996.38
P140	38.829	120.693	-21.9±0.8	-4.2±0.7	-0.08	974	2.8	2006.55
P141	39.047	120.386	-21.7±1.0	-3.9±0.8	0.20	534	2.6	2006.80
P143	38.760	119.765	-22.4±1.2	-4.0±0.9	-0.02	253	1.6	2007.72
P144	39.467	120.893	-22.3±0.9	-4.8±0.9	-0.05	545	1.5	2007.82
P146	39.338	120.537	-22.1±0.7	-4.3±0.7	-0.08	880	2.7	2006.63
P208	39.109	122.304	-22.9±0.7	-5.3±0.6	0.01	1122	3.1	2006.20
P259	37.433	121.101	-22.2±0.7	-3.2±0.6	-0.02	1342	3.8	2005.57
P260	37.711	121.084	-23.3±0.8	-4.2±0.7	-0.03	823	2.4	2005.56
P265	38.530	121.954	-22.9±0.7	-4.2±0.6	-0.17	1276	3.7	2005.65
P267	38.380	121.823	-22.2±0.9	-3.7±0.8	0.43	1385	4.1	2005.26
P268	38.474	121.646	-24.7±0.9	-4.4±0.5	-0.16	1439	4.1	2005.27
P270	39.244	122.055	-23.0±0.6	-5.6±0.6	0.03	1253	4.0	2005.38
P271	38.657	121.715	-23.6±0.6	-4.8±0.5	-0.10	1758	4.9	2004.44
P272	39.146	121.943	-22.7±0.7	-5.8±0.7	0.12	1263	3.5	2005.82
P273	38.116	121.388	-22.9±1.1	-5.2±0.7	-0.09	1265	3.5	2005.82
P274	38.283	121.461	-24.9±1.2	-6.1±1.0	0.02	1263	3.5	2005.82
P275	38.322	121.215	-23.1±0.8	-4.1±0.7	-0.07	1020	2.8	2006.54
P276	38.645	121.095	-23.1±0.6	-4.5±0.6	-0.08	1223	3.5	2005.88
P305	37.352	120.197	-22.7±0.6	-3.2±0.5	-0.12	1359	3.8	2005.56
P306	37.795	120.644	-23.4±0.8	-3.5±0.6	-0.20	995	2.8	2006.53
P309	38.090	120.951	-23.7±0.7	-3.6±0.6	-0.08	1147	3.2	2006.13
P310	38.736	120.334	-21.8±0.8	-4.2±0.7	0.01	919	2.8	2006.56
P725	37.089	119.746	-22.6±0.8	-1.9±0.7	-0.08	718	2.1	2007.25

North and east velocity components  $V_n$  and  $V_e$  in units of mm yr<sup>-1</sup>, relative to ITRF2005. The correlation coefficient specifies the correlation between the north and east velocity variances and should be used to reconstruct their covariance. Station days indicates the number of days used to estimate a station's velocity. Time specifies the interval in years spanned by the GPS data, beginning with the time of the first observation used to define the time series. Corrections for the motion of the ITRF2005 origin relative to Earth's center-of-mass have not been made to these velocities. Station velocities are from GIPSY analysis of GPS code-phase data at the University of Wisconsin-Madison, current through May 10, 2009.



Table 2: GPS station information: Pacific plate

Site code	Lat. °N	Long. °E	$V_e$ mm yr <sup>-1</sup>	$V_n$ mm yr <sup>-1</sup>	Corr. coeff.	Station days	Time yrs	First obs.
1098	24.290	153.979	-71.7±0.7	24.0±0.5	0.12	1916	6.4	2002.94
ASPA	-14.326	189.278	-64.2±0.7	33.8±0.5	-0.15	2448	7.7	2001.61
CHAT	-43.956	183.434	-40.5±0.5	33.3±0.4	0.02	4862	13.6	1995.76
CKIS	-21.201	200.199	-62.0±0.5	34.4±0.4	-0.12	2536	7.7	2001.69
CLAR	18.341	245.265	-58.2±2.8	23.2±2.4	0.00	25	3.1	1997.85
FALE	-13.832	188.000	-64.5±0.7	33.1±0.5	-0.06	1475	10.4	1999.00
GUAX	28.884	241.710	-46.7±0.7	24.7±0.6	-0.07	942	4.2	2001.05
HILO	19.719	204.947	-63.0±0.4	35.6±0.4	0.03	2806	10.4	1999.00
HNLC	21.303	202.135	-62.9±0.5	34.7±0.4	0.12	2964	10.4	1999.00
KIRI	1.355	172.923	-67.9±0.6	31.0±0.5	0.10	2227	6.8	2002.58
KOK1	21.984	200.242	-62.1±0.4	35.2±0.4	0.04	3856	11.7	1996.10
KOKB	22.126	200.335	-60.8±0.6	34.2±0.4	0.11	5279	16.3	1993.02
KWJ1	8.722	167.730	-69.3±1.0	29.4±0.8	0.02	1796	6.3	1996.21
MAJB	7.119	171.365	-70.1±1.5	30.1±0.9	0.05	607	2.0	2007.39
MARC	24.290	153.979	-72.8±1.0	23.1±1.0	-0.01	1555	4.8	1995.54
MAUI	20.707	203.743	-62.2±0.5	34.7±0.3	0.08	3232	10.4	1999.00
MKEA	19.801	204.544	-64.1±0.5	35.2±0.4	-0.05	4349	12.6	1996.75
MAJU	7.119	171.365	-70.1±1.3	29.9±0.9	0.04	622	2.0	2007.39
NAUR	-0.552	166.926	-67.1±0.6	29.2±0.5	0.10	1612	5.9	2003.49
PAMA	-17.567	210.425	-62.9±1.7	29.2±1.8	0.02	757	4.2	1993.00
POHN	6.960	158.210	-69.1±0.9	25.2±0.8	0.08	1979	6.0	2003.33
SAMO	-13.849	188.262	-65.0±0.9	33.2±0.4	-0.03	2500	7.9	2001.50
SOCC	18.728	249.055	-54.2±0.7	21.0±0.9	0.00	40	7.3	1997.84
TAHT	-17.577	210.394	-64.9±1.1	33.6±0.6	-0.03	1493	5.3	2004.00
THTI	-17.577	210.394	-65.7±0.7	34.2±0.4	-0.11	3354	10.9	1998.42
TRUK	7.447	151.887	-70.0±1.2	24.5±0.5	0.07	1150	6.8	1995.93
TUVA	-8.525	179.197	-64.1±0.7	32.1±0.4	0.06	2281	7.4	2001.91

Information about the contents of each column is given in the footnotes for Table 1.

Table 3: GPS station information: Deforming region

Site code	Lat. °N	Long. °W	$V_e$ mm yr <sup>-1</sup>	$V_n$ mm yr <sup>-1</sup>	Corr. coeff.	Station days	Time yrs	First obs.
0508	35.855	120.799	-44.0±3.3	24.7±3.6	0.00	13	3.0	2004.54
0509	35.992	121.484	-35.9±1.4	23.7±1.4	0.00	7	10.4	1994.17
05QJ	35.948	120.878	-41.9±3.2	23.7±3.0	0.00	15	3.0	2004.54
05RH	36.049	120.965	-40.6±1.4	20.7±1.0	0.00	13	2.8	2004.74
05SH	36.153	120.973	-42.6±2.2	23.9±1.5	0.00	15	4.5	2003.05
05SK	36.178	120.691	-19.2±2.4	0.1±1.7	0.00	21	4.5	2003.04
05UH	36.410	120.996	-24.8±0.9	-1.1±0.6	0.00	12	13.9	1993.66
05WF	36.696	121.270	-29.1±4.1	7.3±3.4	0.00	4	2.7	2004.87
05YF	36.793	121.325	-21.5±4.5	-0.5±2.3	0.00	4	2.7	2004.87
AKRS	36.304	120.706	-21.0±2.5	-3.8±1.5	0.00	13	4.1	2003.40
ALVS	36.363	121.226	-39.8±2.2	21.2±1.3	0.00	14	4.5	2003.03
BITT	36.417	120.982	-23.4±2.4	-0.7±1.6	0.00	15	4.1	2003.38
BLAN	35.665	121.284	-38.5±0.4	25.9±0.5	0.00	44	10.1	1994.18
CALL	36.610	121.064	-19.9±0.8	-2.1±0.6	0.34	1030	4.8	2004.57
CAND	35.939	120.434	-23.6±1.6	7.7±2.1	-0.85	3019	9.7	1999.63
CANX	36.413	120.782	-21.5±1.2	-1.1±0.7	0.00	16	8.6	1998.88
CARR	35.888	120.431	-33.1±0.8	17.8±0.4	-0.08	2810	8.9	1994.41
CHLN	36.448	121.195	-39.6±1.4	22.9±0.8	0.00	6	8.7	1998.88
CRBT	35.792	120.751	-38.6±0.6	21.7±0.5	0.32	2372	7.7	2001.70
CRVO	36.445	120.481	-20.2±2.4	0.2±1.2	0.00	5	5.7	1998.88
CVM1	36.473	120.580	-20.7±2.5	-0.9±1.5	0.00	5	5.7	1998.88
DTOG	36.113	120.585	-28.1±2.6	-4.5±2.1	0.00	12	4.1	2003.40
EADE	36.081	120.920	-43.4±2.5	22.1±2.0	0.00	14	4.1	2003.40
GR8V	36.399	120.416	-22.0±0.8	-2.8±0.5	0.27	2174	6.1	2003.04
GRIG	36.029	120.864	-45.0±2.5	22.8±2.4	0.00	16	4.0	2003.41
GRSW	36.503	120.729	-20.0±1.7	-4.0±1.1	0.00	15	6.1	1998.88
HEPS	36.315	120.825	-20.8±2.0	-0.5±1.2	0.00	5	5.7	1998.88
HNDZ	36.363	120.786	-20.5±2.7	-2.1±1.4	0.00	11	4.1	2003.40
HOGS	35.867	120.479	-34.7±1.3	19.3±1.3	-0.63	1353	4.7	2001.53
HOME	36.293	120.989	-40.4±2.5	21.1±1.5	0.00	15	4.1	2003.38
HUNT	35.881	120.402	-25.8±2.3	7.2±2.4	-0.92	2453	7.7	2001.60
LAND	35.900	120.473	-34.2±1.5	19.1±1.4	-0.86	3052	9.7	1999.65
LEY_	36.453	120.894	-21.5±1.3	-1.0±0.9	0.00	9	8.7	1998.88
LOWS	35.829	120.594	-37.4±0.6	21.0±0.5	-0.24	2441	7.8	2001.59
MADS	36.163	120.870	-42.2±2.3	21.1±1.3	0.00	12	4.4	2003.05
MASW	35.833	120.443	-35.3±1.0	18.5±1.6	-0.73	2437	7.8	2001.60
MEE1	36.187	120.759	-23.1±0.6	-1.5±0.5	-0.06	2098	6.3	2003.03
MEE2	36.181	120.767	-40.8±0.6	21.1±0.5	-0.21	2033	6.3	2003.03
MEE3	36.186	120.806	-41.4±2.3	19.4±1.6	0.00	12	4.4	2003.05
MIDA	35.922	120.459	-22.5±1.6	8.8±2.8	-0.78	3045	9.7	1999.65
MNMC	35.970	120.434	-20.9±0.9	5.4±2.0	-0.64	2454	7.8	2001.59
NINO	36.246	121.035	-40.5±2.3	22.5±1.4	0.00	15	4.4	2003.06
NWID	36.419	120.673	-21.3±2.6	-2.1±1.4	0.00	11	4.1	2003.41

Site code	Lat. °N	Long. °W	$V_e$ mm yr <sup>-1</sup>	$V_n$ mm yr <sup>-1</sup>	Corr. coeff.	Station days	Time yrs	First obs.
P067	35.552	121.003	-39.5±0.8	26.6±1.5	0.53	1819	5.3	2004.03
P171	36.486	121.793	-40.2±0.7	24.5±0.5	0.22	1640	4.7	2004.68
P172	36.228	121.767	-42.6±1.4	24.7±1.1	-0.12	379	1.1	2008.31
P173	35.946	121.290	-39.9±1.4	24.6±1.2	0.22	282	0.8	2008.58
P174	36.302	121.051	-40.2±0.8	22.3±0.8	0.06	817	2.3	2007.07
P175	36.426	121.135	-40.8±0.8	22.5±0.6	-0.10	1063	3.0	2006.38
P180	36.293	121.403	-39.2±1.1	22.4±0.9	-0.11	833	2.3	2007.06
P210	36.816	121.732	-40.5±0.6	21.0±0.6	-0.00	1393	4.0	2005.40
P211	36.879	121.698	-39.2±0.8	21.1±0.8	-0.01	703	2.1	2007.22
P216	37.002	121.726	-35.5±0.8	16.3±0.8	-0.01	773	2.1	2007.22
P231	36.622	121.905	-40.3±1.0	24.2±1.0	-0.35	882	2.4	2006.92
P232	36.724	121.579	-40.1±0.8	22.6±0.7	-0.08	770	2.1	2007.23
P233	36.800	121.420	-29.4±0.8	13.1±0.7	-0.00	981	2.7	2006.64
P234	36.859	121.591	-38.1±0.8	19.9±0.7	-0.04	1016	2.8	2006.53
P235	36.814	121.542	-38.7±0.8	22.1±0.8	-0.04	692	1.9	2007.45
P236	36.904	121.554	-34.4±0.7	13.7±0.6	-0.08	1133	3.6	2005.80
P237	36.637	121.387	-39.5±0.8	22.2±0.7	-0.09	808	2.2	2007.13
P238	36.849	121.453	-28.3±1.1	11.9±0.8	-0.38	1116	3.1	2006.27
P240	37.008	121.542	-32.1±0.7	11.5±0.6	0.09	1275	4.0	2005.40
P242	36.954	121.463	-32.0±0.8	10.2±1.1	-0.24	1537	4.4	2004.96
P243	36.918	121.335	-25.3±0.8	-2.4±0.8	-0.03	692	2.0	2007.38
P244	37.011	121.355	-26.0±0.7	-1.9±0.6	-0.07	1240	3.5	2005.88
P247	36.560	121.188	-39.7±1.0	22.6±0.7	0.12	1061	3.0	2006.40
P250	36.950	121.268	-24.7±0.8	-1.4±0.7	-0.03	710	2.0	2007.37
P251	36.811	121.348	-24.2±0.7	1.8±0.6	0.06	975	3.1	2006.27
P252	37.170	121.058	-23.4±0.6	-3.1±0.6	-0.08	1169	3.5	2005.86
P259	37.433	121.101	-22.2±0.7	-3.2±0.6	-0.02	1342	3.8	2005.57
P278	35.711	121.061	-40.7±0.7	20.7±0.9	-0.00	1751	5.3	2004.09
P279	35.791	121.062	-40.7±0.9	22.1±0.8	0.05	618	1.7	2007.64
P280	35.544	120.348	-36.1±0.9	19.0±0.6	0.02	1039	2.9	2006.47
P281	35.841	120.389	-33.1±2.6	20.0±2.8	-0.87	1365	4.5	2004.86
P282	35.838	120.345	-24.6±2.8	6.3±1.0	-0.69	1420	4.5	2004.84
P283	35.807	120.285	-24.7±1.7	7.0±0.5	-0.28	1587	4.5	2004.84
P284	35.933	120.907	-39.6±0.7	20.9±0.6	0.09	1520	4.2	2005.10
P285	36.417	120.981	-23.3±0.8	1.0±0.6	-0.03	1012	2.8	2006.53
P286	36.516	120.853	-21.7±0.9	-1.1±0.9	-0.07	618	1.7	2007.64
P287	36.025	120.698	-40.3±0.6	20.4±0.6	0.03	1476	4.3	2005.10
P288	36.140	120.879	-40.6±0.7	21.8±0.6	-0.12	1138	3.2	2006.14
P289	36.107	120.749	-40.1±0.8	21.4±0.7	-0.01	831	2.3	2007.07
P290	36.179	120.728	-21.1±0.7	-0.5±0.6	-0.01	1141	3.2	2006.15
P291	35.923	120.645	-37.9±0.8	21.5±0.8	-0.06	626	1.7	2007.64
P292	36.008	120.475	-19.7±1.3	6.3±1.3	0.22	451	1.2	2008.11
P293	36.089	120.543	-19.7±0.9	1.9±0.7	-0.05	905	2.6	2006.76
P294	36.123	120.440	-21.0±0.6	1.4±0.6	0.01	1069	3.0	2006.38
P295	35.697	120.842	-39.1±0.5	20.7±0.6	0.17	1771	5.3	2004.03

Site code	Lat. °N	Long. °W	$V_e$ mm yr <sup>-1</sup>	$V_n$ mm yr <sup>-1</sup>	Corr. coeff.	Station days	Time yrs	First obs.
P296	36.052	120.364	-20.2±0.8	2.6±0.7	0.12	920	2.6	2006.77
P297	35.974	120.552	-38.1±0.7	21.5±0.7	-0.26	1087	3.6	2005.80
P298	36.016	120.294	-21.0±0.7	2.6±0.6	0.32	1187	3.4	2006.00
P300	36.304	120.277	-21.0±1.0	0.4±1.0	0.56	1508	4.4	2004.95
P301	36.806	120.743	-22.1±0.6	-3.1±0.5	-0.05	1568	4.4	2004.96
P302	36.635	120.619	-20.5±0.8	-1.5±0.6	0.24	1399	4.4	2004.96
P303	37.054	120.705	-23.5±0.7	-2.9±0.6	0.01	1268	3.8	2005.57
P304	36.739	120.357	-22.8±0.6	-2.6±0.6	0.16	1616	5.0	2004.33
P514	35.011	120.410	-40.5±0.8	22.2±0.7	0.36	993	2.8	2006.57
P516	35.106	120.383	-39.4±0.9	22.1±0.7	0.23	1062	3.3	2006.10
P523	35.304	120.860	-40.3±0.7	23.9±0.6	-0.07	1118	3.3	2006.09
P524	35.166	120.591	-40.3±0.9	23.1±0.7	0.03	725	2.0	2007.05
P526	35.636	120.870	-38.5±0.7	20.0±0.8	0.13	1815	5.3	2004.03
P527	35.754	120.605	-37.0±0.8	20.3±0.7	-0.06	973	2.7	2006.66
P529	35.440	120.354	-36.2±0.8	20.4±0.7	0.06	936	2.9	2006.47
P530	35.625	120.480	-36.5±0.6	21.9±0.6	0.15	1371	3.8	2005.52
P531	35.793	120.537	-37.0±0.8	20.7±0.7	-0.04	834	2.3	2007.05
P532	35.634	120.267	-33.4±0.7	16.1±0.6	0.24	1643	4.6	2004.77
P533	35.748	120.371	-33.4±0.9	18.3±0.6	-0.03	1061	3.0	2006.36
P535	35.235	120.101	-37.0±0.8	17.5±0.7	0.05	939	2.6	2006.72
P536	35.280	120.025	-35.6±0.8	16.0±0.6	-0.03	1077	3.0	2006.34
P537	35.317	119.935	-33.8±0.8	13.2±0.6	0.06	1080	3.0	2006.34
P538	35.534	120.112	-32.6±0.8	12.9±0.6	-0.02	1075	3.0	2006.34
P539	35.703	120.182	-28.1±1.0	8.2±0.5	-0.09	1436	4.6	2004.75
P540	35.801	120.131	-24.8±0.6	4.2±0.6	-0.00	1061	3.2	2006.10
P541	35.687	120.001	-24.9±0.6	4.8±0.5	-0.05	1130	3.8	2005.51
P542	35.689	120.293	-33.7±1.0	15.3±0.9	0.17	445	1.2	2008.13
P543	35.319	119.713	-27.8±0.9	7.2±0.7	0.19	1036	2.9	2006.47
P544	35.731	119.738	-21.0±0.7	0.3±0.6	-0.11	1101	3.4	2005.95
P545	35.500	119.536	-23.7±1.1	3.0±1.0	0.25	548	1.5	2007.83
P546	35.928	120.155	-21.8±0.7	3.2±0.6	-0.03	1152	3.3	2006.09
P547	35.935	119.909	-21.1±0.7	2.1±0.7	0.04	1095	3.4	2005.95
P552	35.687	120.245	-33.1±1.1	13.9±1.0	0.13	446	1.2	2008.12
P564	35.623	119.349	-25.4±1.1	5.5±1.4	0.09	884	2.5	2006.84
P576	35.670	120.970	-40.5±1.3	21.0±2.3	0.64	1643	5.3	2004.04
P602	35.729	120.228	-28.0±1.1	8.8±1.0	0.03	448	1.2	2008.12
PANC	36.698	120.739	-21.4±1.2	-1.8±0.7	0.00	22	8.6	1998.88
PFYF	36.202	120.736	-22.7±0.8	-3.3±0.8	0.00	17	4.4	2003.06
PHEL	36.220	120.488	-24.3±2.5	-4.8±1.4	0.00	13	4.1	2003.40
PKDB	35.945	120.542	-34.7±1.4	20.3±0.9	-0.78	4085	12.6	1996.72
POMM	35.920	120.478	-34.1±2.3	17.6±1.3	-0.89	3123	9.7	1999.64
QCYN	36.161	121.137	-39.8±0.5	22.3±0.5	0.03	2231	6.3	2003.05
RED_	36.685	120.934	-21.5±1.6	-0.5±1.1	0.00	8	8.7	1998.88
RIST	36.304	120.898	-40.4±2.4	19.8±1.5	0.00	14	4.1	2003.39
RNCH	35.900	120.525	-36.5±1.8	20.1±1.2	-0.56	2413	7.8	2001.60

Site code	Lat. °N	Long. °W	$V_e$ mm yr <sup>-1</sup>	$V_n$ mm yr <sup>-1</sup>	Corr. coeff.	Station days	Time yrs	First obs.
RNDA	36.279	121.318	-40.3±2.4	23.4±1.4	0.00	14	4.1	2003.41
SANS	36.434	121.034	-40.4±2.5	21.0±1.4	0.00	13	4.1	2003.39
SAOB	36.765	121.447	-40.5±0.5	23.8±0.5	-0.22	3674	11.8	1997.52
SBEN	36.370	120.645	-20.8±2.5	-5.1±1.3	0.00	10	4.0	2003.42
SERP	36.325	120.549	-21.2±2.5	-4.1±2.2	0.00	9	4.1	2003.42
SHAD	36.030	120.682	-42.6±1.5	25.9±2.1	0.00	13	8.7	1998.88
SMOK	36.537	121.000	-20.4±1.9	-1.6±1.3	0.00	5	5.7	1998.88
SPAR	36.151	120.940	-42.2±2.3	21.6±2.0	0.00	13	4.4	2003.05
STRO	36.188	120.662	-21.9±2.3	-4.6±1.3	0.00	13	4.4	2003.05
SWTR	36.228	120.923	-40.3±1.5	22.2±1.2	0.00	7	8.7	1998.88
TBLP	35.917	120.360	-25.2±1.3	5.1±1.2	-0.60	2391	7.6	2001.74
TIGA	36.794	120.923	-22.1±1.4	-1.4±0.8	0.00	9	8.7	1998.88
TLY1	36.346	120.944	-40.5±2.5	20.9±1.5	0.00	13	4.1	2003.39
TLY2	36.347	120.916	-21.9±2.4	-1.3±1.8	0.00	14	4.1	2003.39
TUMY	36.611	120.665	-21.1±0.4	-2.4±0.4	0.00	24	8.6	1998.88
USLO	35.312	120.661	-39.7±0.4	24.2±0.4	0.13	3034	8.6	2000.74
WFLG	35.947	121.065	-39.3±2.5	21.2±2.6	0.00	12	4.1	2003.41

Information about the contents of each column is given in the footnotes for Table 1.